This document is confidential and is proprietary to the American Chemical Society and its authors. Do not copy or disclose without written permission. If you have received this item in error, notify the sender and delete all copies.

Nanoparticles conjugated with photo-cleavable linkers for the intracellular delivery of biomolecules

Journal:	*Bioconjugate Chemistry*
Manuscript ID	bc-2017-008207.R1
Manuscript Type:	Communication
Date Submitted by the Author:	n/a
Complete List of Authors:	Jiménez-Balsa, Adrián; CNC.IBILI, Pinto, Sandra; Center of Neurosciences and Cell Biology, Quartin, Emanuel; CNC.IBILI Lino, Miguel; CNC.IBILI Francisco, Vitor; CNC.IBILI Ferreira, Lino; Center for Neuroscience and Cell Biology,

SCHOLARONE™
Manuscripts

Nanoparticles conjugated with photo-cleavable linkers for the intracellular delivery of biomolecules

A. Jiménez-Balsa,[†] S. Pinto,[†,‡] E. Quartin,[†,‡] M. M. Lino,[†,‡] V. Francisco,[†,‡] and L. Ferreira[†,‡,*]

[†]CNC-Center for Neurosciences and Cell Biology, University of Coimbra, 3000, Coimbra, Portugal
[‡]Faculty of Medicine, University of Coimbra, 3000, Coimbra, Portugal
* E-mail: lino@uc-biotech.pt. Phone: (+351)-231249170. Fax: (+351)-231249179.

We report the synthesis and characterization of photo-triggerable polymeric nanoparticles (NPs) for the intracellular delivery of small molecules and proteins to modulate cell activity. For that purpose, several photo-cleavable linkers have been prepared providing diverse functional groups as anchoring points for biomolecules.

The advent of precision and regenerative medicine requires the development of novel systems for on-demand delivery of biomolecules into cells in order to modulate their activity/identity.[1-3] Such triggerable systems should allow precise control of the timing and spatial release of the biomolecules. Triggerable NPs may respond to endogenous stimuli such as pH,[4] enzymatic activity,[5] redox environment[6, 7] but also exogenous factors such as magnetic,[8] ultrasound,[9] temperature[10] and light.[11] The remote activation of the NP may enable repeated and reproducible dosing of the drug, reducing risks associated with toxicity while increasing efficacy. Light offers some advantages relatively to other external triggers such as spatial control (delimited by the light beam) and release control of multiple biomolecules using different wavelengths[12-14]. A significant number of light-triggerable NPs is constituted by compounds that respond to UV light[15, 16], since it is a high-energy radiation capable of inducing conformational changes or break covalent bonds. UV light-triggerable NPs may have special use skin and eye applications, but also in surgical procedures using laparoscopic techniques.[17, 18] A variety of formulations for drug delivery have included photocleavage linkers (PCL) that can be cleaved upon light irradiation and release the biomolecules.[19, 20] Among these photosensitive compounds, the ortho-nitrobenzyl-based and their dimethoxy derivatives[21] are by far the most studied. However, very few NP formulations are (i) formed by components that can be eliminated by the human body (and thus avoiding the use of inorganic materials such as gold and iron oxide which raise problems regarding toxicity and clearance), (ii) have the ability to efficiently penetrate the cell membrane and accumulate in the cell cytoplasm and (iii) have the ability to release the cargo only after light activation (and thus without leaching) without damaging the cell. Indeed, it is difficult to combine

all these features in the same system. This requires the development of NPs that are easily taken up by cells and accumulate in the cytoplasm and the development of PCLs that can be photocleaved by light in order to release the cargo only after light exposure (therefore preventing cargo delivery in a passive way, i.e., by diffusion). Such a system would grant us the unprecedented ability to spatio-temporally control the release of biomolecules within cells. Few examples of heterobifunctional PCLs are reported in the literature.[22-24] In addition, most PCLs prepared by synthesis in solution are obtained either from expensive starting materials, or after challenging and/or very low-yield synthesis.[23-24]

Herein, we report a UV/blue-triggerable polymeric NP that may have potential application for the intracellular delivery of small molecules and proteins. We have synthesized a set of PCLs that are characterized by heterobifunctionality, orthogonality and diversity of functional groups (e.g. amine, acid, and isothiocyanate) to covalently conjugate the biomolecules. After covalent ligation of the bioactive compound to the PCL, the resulting conjugate was attached to the polymeric carrier by click chemistry, under mild conditions. The core of the NP is formed by components that have the ability to efficiently penetrate the cell membrane and accumulate in the cell cytoplasm[25, 26] while the cargo is covalently immobilized to the NP by a PCL.

To conjugate the different cargos (i.e. proteins and small molecules) to the NP we have developed a set of PCLs from relatively non-expensive starting materials and in high yield (Scheme 1). All the PCLs responded to UV light (365 nm, ≈100 mW/cm^2) after solubilisation in aqueous solutions or dimethylsulfoxide (Fig. 1 and Figs. S1 and S2, ESI†), as monitored by spectrophotometry. The photocleavage of PCLs was also confirmed by ^{1}H-NMR in d^6-DMSO (Fig. 1C and Fig. S3, ESI†). As expected, the results from NMR and spectrophotometry show that PCLs are photo-cleavable in a concentration-dependent manner. The increase in the concentration of PCL-3 from 0.35 mM to 63 mM strongly decreases the photocleavage percentage as measured by UV-Vis (Fig. 1C) and NMR (Fig. 1C and Fig. S3-B). Similar photocleavage kinetics were obtained in both experiments for concentrations of PCLs of 63 to 89 mM (Fig. 1C and Fig. S4, ESI†). Our results further show that the photo-cleavage

kinetics is not affected by the measuring technique. Results obtained by UV-Vis (Fig. S2-B) and NMR (Fig. S3-A; disappearance of peak 4 in the NMR spectrum) studies for PCL-1 shown similar photo-cleavage (100%) upon irradiation of samples for 10 min with a UV-lamp, under diluted conditions (0.35 mM). Overall, our results highlight the importance of the PCL concentration in the photo-dissociation process. The three PCLs had similar photocleavage constants (PCL-1: -0.0201 min^{-1}, PCL-2: -0.0247 min^{-1}, PCL-3: -0.0147 min^{-1}) (Fig. S4, ESI†), which are in line with previous studies showing that chemical modifications away from the aromatic ring have little effect in PCL photo-cleavage kinetics.[27] Importantly, a conventional blue laser (405 nm, 80 mW) can replace the UV light to induce the photo-cleavage of the PCLs (Fig. S5, ESI†).

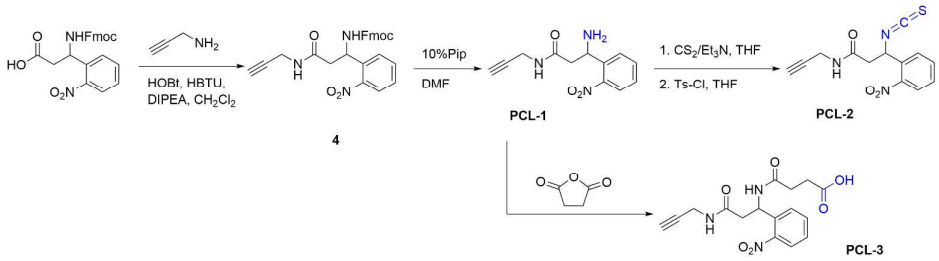

Scheme 1 Synthesis of the different PC-linkers (PCL), ready for the conjugation with activated acids (**PCL-1**), amines or other nucleophiles (**PCL-2**), or right after activation (i.e. EDC/NHS) also with amines or other nucleophiles (**PCL-3**). Reactive groups are shown in blue.

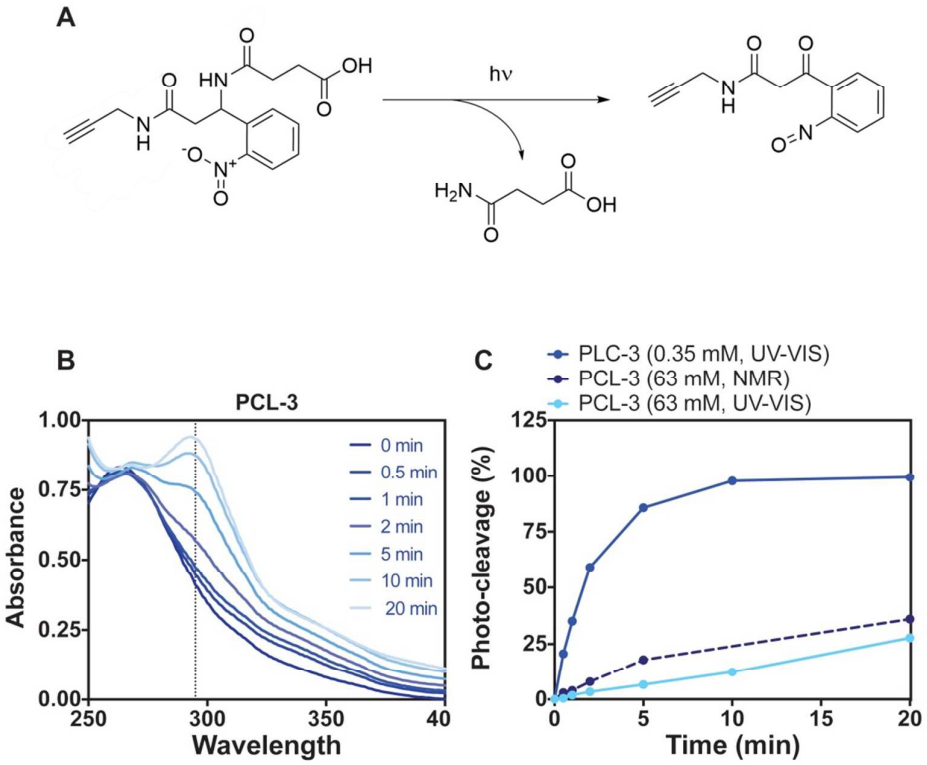

Fig. 1 Time-course for the photocleavage of **PCL-3** by UV radiation in aqueous solution. (A) Schematic representation of the photocleavage of **PCL-3**. (B) Absorbance spectra of **PCL-3** aqueous solution (350 μM in PBS) after exposure to a UV lamp for different period of times. (C) Percentage of **PCL-3** photocleavage as monitored by absorbance and ^{1}H-NMR. Absorbance monitored at 295 nm was normalised by the maximum absorbance at that peak (approximately 20 min after UV radiation). In case of ^{1}H-NMR analyses, the photocleavage was calculated from the ratio of peak area at 5.5 ppm and peak area at 0 ppm (see experimental section).

To demonstrate the value of the synthesized PCLs we have conjugated them to NPs followed by their reaction with biomolecules. For proof of concept we have used lysozyme since it is relatively easy to follow its enzymatic activity. The NPs were prepared by complex coacervation, *i.e.*, through the electrostatic interaction of polyethylenimine (PEI, polycation) and dextran sulfate (DS, polyanion) using zinc sulfate as a physical crosslinker.[26] The PEI-DS NPs **6** (Scheme 2, bottom part) had a diameter of 192 ± 6.6 nm and positive net charge (21.2 ± 1.8 mV) and rapidly accumulate in the cell cytoplasm.[26] To conjugate the NP with the lysozyme, the enzyme was initially reacted with PCL-2 (Scheme 2, upper part) in phosphate buffer solution (PBS) pH 7.4, in a ratio of 1 lysozyme for 20

molecules of PCL-2. The resulting conjugate (Lyso-PCL, **5**, Scheme 2) was purified by dialysis, and characterized by size-exclusion chromatography (Fig. 2A) and enzymatic activity (Fig. 2B), before and after light activation. Our results indicate that the conjugation of PCL-2 to lysozyme as well as the UV irradiation did not affect enzyme activity (Fig. 2B). PEI-DS NPs were then coated with activated azido-PEG4-COOH (**7**, Scheme 2). The azide groups on the NPs were quantified by reaction with an alkyne-fluorescein compound followed by dialysis and fluorescence measurement (see ESI†). PEI-DS NPs showed an average of 1.5 nmol N_3 per mg of NP. The Lyso-PCL conjugate (10 equiv.) was then reacted with the azide groups of the polymeric NPs **7** by CuAAC click chemistry, under mild conditions (Scheme 2). The reaction product **8** (Lyso-NPs) was purified by dialysis and characterized by DLS. NPs with a diameter of 143.2 ± 35.3 nm, zeta potential of +19 ± 0.5 mV and 8.8 μg of protein per mg of NPs were obtained. The decrease in NPs diameter after conjugation with Lyso-PCL is likely justified by re-arrangements of the NPs triggered by electrostatic interactions between the protein and components of the NPs (PEI and DS). To demonstrate the photo-triggerable properties of Lyso-NP formulation, the NPs were irradiated in intervals of 5 min (3 × 5 min), centrifuged, the supernatants freeze-dried and the enzyme activity quantified (Fig. 2C, solid red line). Taking into account the initial concentration of enzyme immobilized per mg of NP (formulation **8**) we estimated that approximately 24% was released. This corresponded to 2.1 μg of lysozyme released per mg of Lyso-NP. Interestingly, the release of lysozyme led to an increase in NP diameter (from 143.2 ± 35.3 nm to 226.7 ± 35.5 nm).

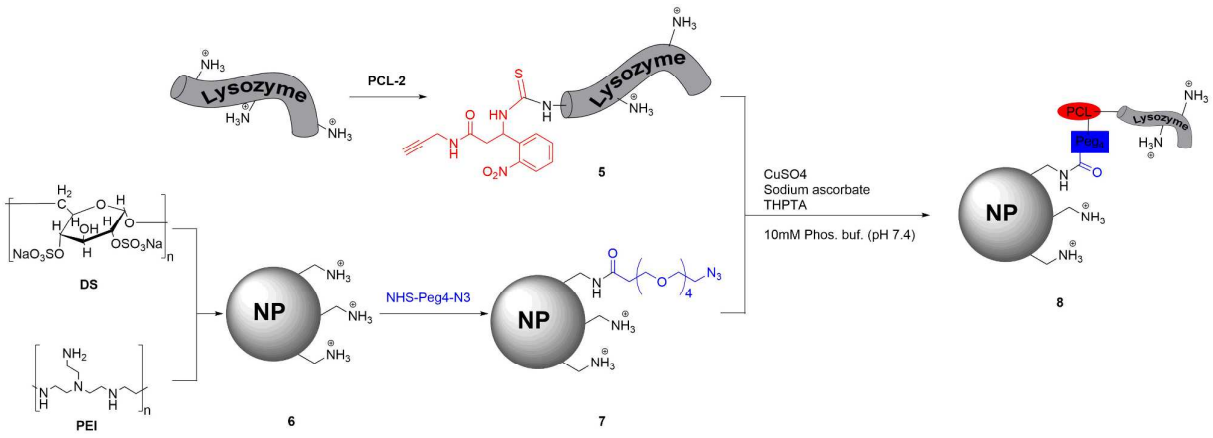

Scheme 2 Lysozyme decorated PEI-DS NPs **8** obtained by bioconjugation of NPs **7** with Lyso-PCL (**5**). Lyso-PLC conjugate results from the functionalization of Lysozyme using **PCL-2**, and PEI-DS NPs **7** are prepared from PEI and DS and consequently decorated at the surface using Azido-PEG4-NHS.

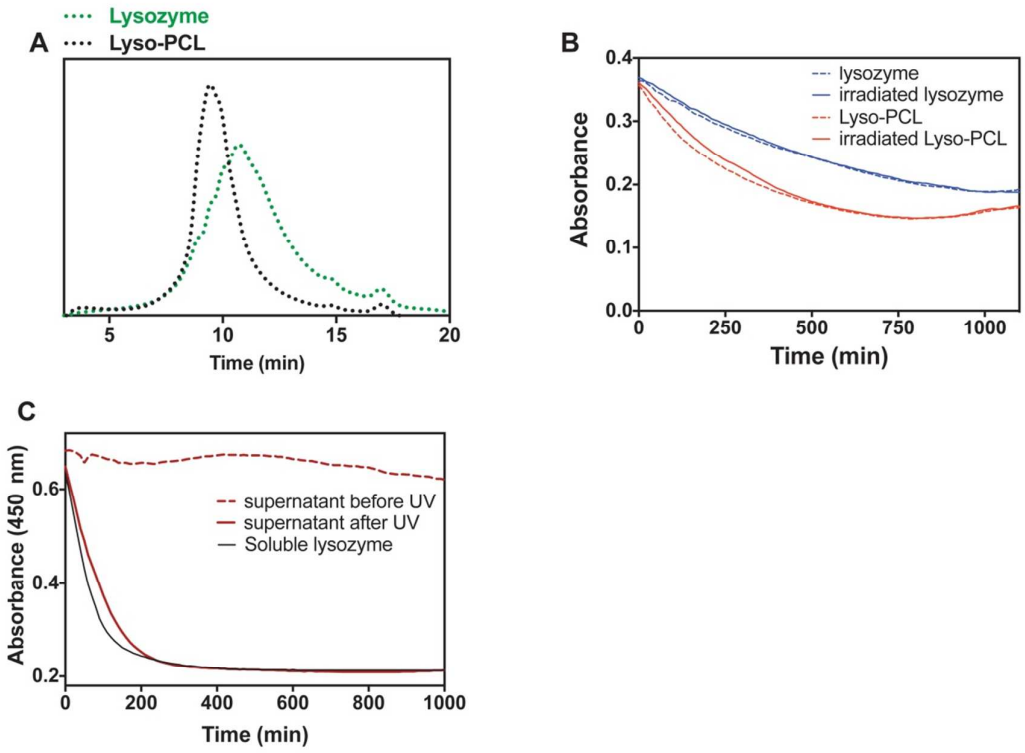

Fig. 2 Light-activatable NPs for the release of lysozyme. (A) HPLC chromatogram traces for native lysozyme (dotted green line) and lysozyme conjugated to **PCL-2** (Lyso-PCL) (dotted black line). (B) Activity for lysozyme and Lyso-PCL. The enzymatic activity of lysozyme was determined using *Micrococcus lysodeikticus* bacterial cells as a substrate. The degradation of the substrate was monitored at 450 nm. Plot displays the average of two replicates per each experimental group. (C) Photorelease of lysozyme from decorated NPs. A suspension of NPs (5 mg/mL, in PBS) was centrifuged and the

enzyme activity of the supernatant evaluated by an enzymatic assay. Then, the pellet of the NPs was resuspended in PBS and irradiated by a UV lamp (see experimental section), centrifuged and the supernatant evaluated by an enzymatic assay. To determine the concentration of active lysozyme released, a calibration with soluble enzyme was performed (plot indicate the enzymatic activity of 200 nM of soluble lysozyme).

To show the versatility of our approach, we have extended the concept to small molecules (Scheme 3). We have chosen all-trans retinoic acid (atRA) as a key cell modulator. atRA is used in the clinic for the treatment of acute promyelocytic leukemia,[28] severe acne and psoriasis[29]. In addition, it is an important differentiation agent of neural stem cells[25, 26] as well as leukemia cells[11]. RA was not immobilized in the surface of PEI:DS NPs (as lysozyme) but immobilized in PEI polymer to increase the amount of immobilized RA and to yield directly NPs (PEI-atRA NPs) due to the hydrophobic properties of RA. Initially, atRA was reacted with PCL-1 to yield conjugate atRA-PCL **9**, which after purification, was confirmed by ^{1}H-NMR (Fig. S6, ESI†). Our results show that the conjugate is photocleaved by UV light (Fig. S7, ESI†). The atRA-PCL **9** conjugate was then reacted with PEI previously conjugated with an azide-modified poly(ethyleneglycol) (Scheme 3, compound **10,** *ca.* 50 % of the PEI monomeric units have been modified with poly(ethyleneglycol)) using a CuAAC reaction in phosphate buffer saline: DMSO (3:1) solution (Scheme 3) (Fig. S8, ESI†). The modified polymer **11** was purified by dialysis, and the degree of substitution of atRA in PEI was determined by ^{1}H NMR. The ratio of the peak area assigned to two protons of the PCL aromatic ring (7.75 and 8.15) with the peak area assigned to protons **b** of PEG-modified PEI (Fig S8-B, ESI†) indicate that the degree of substitution of atRA was approximately 4%. The resulting conjugate is sensitive to UV light (Fig. 3B). During dialysis, we obtained PEI-atRA NPs. These NPs were formed likely due to the interaction of RA hydrophobic moieties, among other physico-chemical forces. The PEI-atRA NPs presented an average size of 142.1 ± 34.9 nm (Fig. S9, ESI†), zeta potential of -11.8 ± 2.7 mV (Fig. S9, ESI†) and 137 μg of RA per mg of NPs. In addition, the PEI-atRA NPs showed relatively good stability after

suspension in cell culture media (RPMI-1640 medium supplemented with 1% fetal bovine serum, Fig. S10, ESI†).

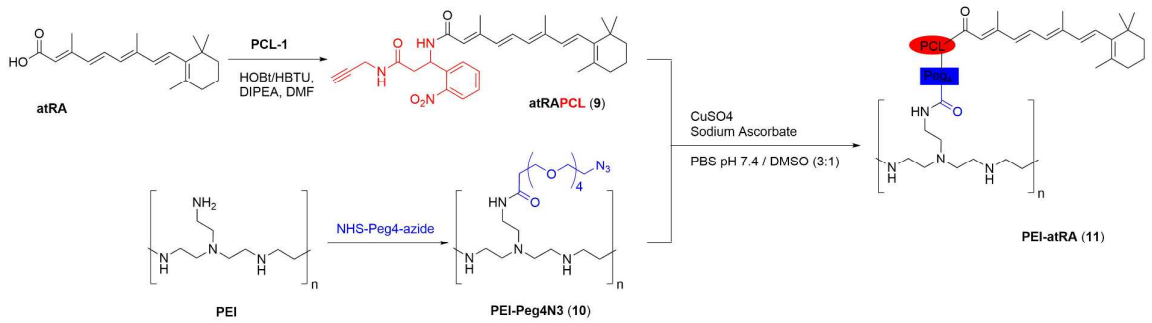

Scheme 3 (a) Preparation of the conjugate atRA-PCL from **PCL-1** and all-trans retinoic acid (atRA). (b) Pegylated PEI synthesis using a pre-activated Azido-PEG4-NHS. (c) Preparation of the final functionalized polymer PEI-atRA.

Next, we evaluated the atRA release properties of PEI-atRA NPs after light activation. For that purpose, a suspension of PEI-atRA NPs was exposed to UV light, centrifuged, and the supernatant added to a NB4-RARE reporter cell line (the atRA induces the expression of RARE element driving the transcription of the firefly luciferase gene) for 4 h (Fig. 3A). The cells were then washed, cultured for additional 20 h and luciferase levels quantified. Our results show that higher levels of luminescence were observed in cells treated with the supernatant of PEI-atRA NPs after light activation for 1 or 3 min (Fig. 3C), thus indicating high intracellular levels of RA. Then we asked whether the release of RA could be UV light-triggered in cells that internalized PEI-atRA NPs. To confirm that PEI-atRA NPs could be internalized by NB4 cells we performed confocal microscopy analyses (Fig. S11, ESI†). Indeed, fluorescently labelled NPs could be observed in the cell cytoplasm. Next, we transfected NB4-RARE cells with PEI-atRA NPs (10 μg/mL) or soluble RA (10 μM) for 4 h (Fig. 3A). After a washing step, the cells were either activated or not by a UV light for 1 min, cultured for additional 20 h and finally the luciferase levels quantified (Fig. 3D). Although the non-irradiated PEI-atRA NPs were able to induce RA signalling (to the levels of soluble RA), the light activated PEI-atRA NPs were more effective. The induction of RA signalling by PEI-atRA NPs not activated by light indicates that RA molecules immobilized in the surface of the NP, or in PEI molecules disassembled from the NPs

during intracellular trafficking, may trigger RA signalling. This is an issue that deserves further investigation.

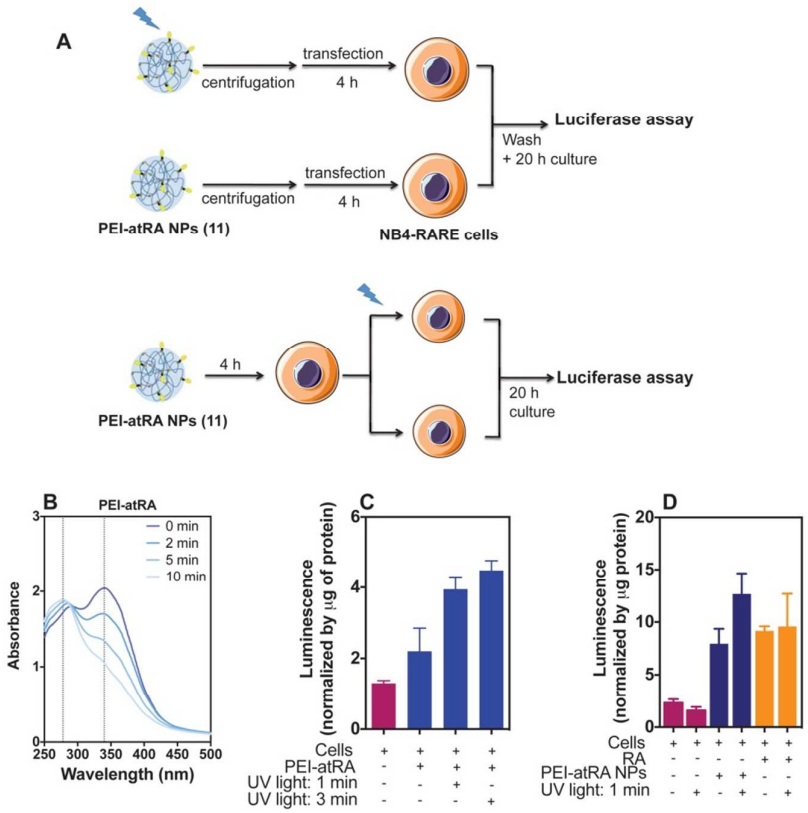

Fig. 3 Light-activatable NP for the release of atRA. (A) Schematic representation of the protocol used to evaluate the release of RA using a RARE luciferase cell line. (B) Absorbance spectra of **PEI-atRA** solution (2 µM, 100 µg/mL in DMSO) after exposure to a UV lamp (365 nm, 100 mW/cm2, 5 cm distance) for different period of times (indicated in the graph). Absorbance at 268 nm is related to **PCL-1** while at 354 nm is related to atRA. (C) Release of RA from **PEI-atRA** was evaluated with a NB4-RARE luciferase cell line. NB4-RARE cells were cultured for 4 h with 10 µg/mL of soluble polymer (PEI-atRA) either or not irradiated prior to addition on cells. The cells were then cultured for 24 h before luciferase luminescence reading. Results are normalized to the mass of protein in each condition. (D) NB4-RARE cells were cultured for 4 h with either 10 µg/ml of PEI-atRA NPs or 10 µM soluble RA and washed before being irradiated or not with 1 min of UV. The cells were then cultured for 20 h before luciferase luminescence reading. Results are normalized to the mass of protein in each condition. In C and D results are average ± SEM, n=3.

In conclusion, we describe a photo-triggerable polymeric NP for on demand delivery of proteins and small molecules. The NP is formed by polymeric components that facilitate cell

internalization and endo-lysosomal escape[25, 26] and a PCL to conjugate a biomolecule. The PCLs have in one end an amine, acid, or isothiocyanate group for the coupling reaction with biomolecules and in the other end a terminal alkyne group to react with the NP by click chemistry. These PCLs compare favourably to other PCLs described in the literature because of their chemical diversity, mild conditions for reaction, high yield (between 70 and 87%), and low cost. The conjugation of the biomolecules to the NPs is performed in aqueous solution and the light activation of the NP has no significant impact in their activity. The application of the photo-triggerable polymeric NP was demonstrated in the intracellular delivery of RA using a leukemic reporter cell line.

The authors declare no competing financial interest.

The authors would like to thank the financial support of FEDER through the program COMPETE and by Portuguese funds through FCT (SFRH/BD/90964/2012 to EQ) (SFRH/BPD/102103/2014 to VF), the EC (ERC project nº 307384, "Nanotrigger"; ERA Chair project ERA@UC (ref: 669088) through European Union´s Horizon 2020 program; both to LF) and Galicia regional funds (through I2C program) for the fellowship to AJ (Ref: POS-A/2013/055). The authors would like to acknowledge the use of the Laboratório de Bio-imagem de Alta Resolução of the Faculty of Medicine of University of Coimbra and the UC-NMR facility.

Notes and references

1. Ferreira, L., Karp, J. M., Nobre, L., and Langer, R. (2008) New opportunities: the use of nanotechnologies to manipulate and track stem cells. *Cell Stem Cell 3*, 136-146.
2. Ambrosone, A., Marchesano, V., Carregal-Romero, S., Intartaglia, D., Parak, W. J., and Tortiglione, C. (2016) Control of Wnt/β-catenin signaling pathway in vivo via light responsive capsules. *ACS Nano 10*, 4828-4834.
3. Santos, T., Boto, C., Saraiva, C. M., Bernardino, L., and Ferreira, L. (2016) Nanomedicine approaches to modulate neural stem cells in brain repair. *Trends Biotechnol. 34*, 437-439.
4. Gao, W., Chan, J. M., and Farokhzad, O. C. (2010) pH-Responsive nanoparticles for drug delivery. *Mol. Pharmaceutics 7*, 1913-1920.

5. Zhu, S., Nih, L., Carmichael, S. T., Lu, Y., and Segura, T. (2015) Enzyme-responsive delivery of multiple proteins with spatiotemporal control. *Adv. Mater. 27*, 3620-3625.
6. Luo, Z., Cai, K., Hu, Y. Zhao, L., Liu, P., Duan, L., and Yang, W. (2011) Mesoporous silica nanoparticles end-capped with collagen: redox-responsive nanoreservoirs for targeted drug delivery. *Angew. Chem. Int. Ed. 50*, 640-643.
7. Wang, Y., Chen, P., and Shen, J. (2006) The development and characterization of a glutathione-sensitive cross-linked polyethylenimine gene vector. *Biomaterials 27*, 5292-5298.
8. Derfus, A. M., von Maltzahn, G., Harris, T. J., Duza, T., Vecchio, K. S., Ruoslahti, E., and Bhatia, S. N. (2007) Remotely Triggered Release from Magnetic Nanoparticles. *Adv. Mater. 19*, 3932-3936.
9. Sirsi, S. R., and Borden, M. A. (2014) State-of-the-art materials for ultrasound-triggered drug delivery. *Adv. Drug Delivery Rev. 72*, 3-14.
10. Kneidl, B., Peller, M., Winter, G., Lindner, L. H., and Hossann, M. (2014) Thermosensitive liposomal drug delivery systems: state of the art review. *Int. J. Nanomed. 9*, 4387-4398.
11. Boto, C., Quartin, E., Cai, Y., Martin-Lorenzo, A., Cenador, M. B. G., Pinto, S., Gupta, R., Enver, T., Sanchez-Garcia, I., Hong, D., and et al. (2017) Prolonged intracellular accumulation of light-inducible nanoparticles in leukemia cells allows their remote activation. *Nat. Commun. 8*, 15204.
12. Azagarsamy, M. A., and Anseth, K. S. (2013) Wavelength-controlled photocleavage for the orthogonal and sequential release of multiple proteins. *Angew. Chem. Int. Ed. 52*, 13803-13807.
13. Priestman, M. A., Sun, L., and Lawrence, D. S. (2011) Dual wavelength photoactivation of cAMP- and cGMP-dependent protein kinase signaling pathways. *ACS Chem. Biol. 6*, 377-384.
14. San Miguel, V., Bochet, C. G., and del Campo, A. (2011) Wavelength-selective caged surfaces: how many functional levels are possible? *J. Am. Chem. Soc. 133*, 5380-5388.
15. Jochum, F. D., and Theato, P. (2013) Temperature- and light-responsive smart polymer materials. *Chem. Soc. Rev. 42*, 7468-7483.
16. Huang, Y., Dong, R., Zhu, X., and Yan, D. (2014) Photo-responsive polymeric micelles. *Soft Matter 10*, 6121-6138.
17. Huu, V. A. N., Luo, J., Zhu, J., Zhu, J., Patel, S., Boone, A., Mahmoud, E., McFearin, C., Olejniczak, J., Lux, C. D., and et al. (2015) Light-responsive nanoparticle depot to control release of a small molecule angiogenesis inhibitor in the posterior segment of the eye. *J. Controlled Release 200*, 71-77.
18. Parani, M., Lokhande, G., Singh, A., and Gaharwar, A. K. (2016) Engineered nanomaterials for infection control and healing acute and chronic wounds. *ACS Appl. Mater. Interfaces 8*, 10049-10069.
19. Jain, P. K., Karunakaran, D., and Friedman, S. H. (2013) Construction of a photoactivated insulin depot. *Angew. Chem. Int. Ed. 52*, 1404-1409.
20. Li, J. M., Lee, W. Y. W., Wu, T. Y., Xu, J. B., Zhang, K. Y., Wong, D. S. H., Li, R., Li, G., and Bian, L. M. (2016) Near-infrared light-triggered release of small molecules for controlled differentiation and long-term tracking of stem cells *in vivo* using upconversion nanoparticles. *Biomaterials 110*, 1-10.
21. Zhao, H., Sterner, E. S., Coughlin, E. B., and Theato, P. (2012) o-Nitrobenzyl alcohol derivatives: opportunities in polymer and materials science. *Macromolecules 45*, 1723-1736.
22. Guillier, F., Orain, D., and Bradley, M. (2000) Linkers and cleavage strategies in solid-phase organic synthesis and combinatorial chemistry. *Chem. Rev. 100*, 3859-3859.
23. Griffin, D. R., Schlosser, J. L., Lam, S. F., Nguyen, T. H., Maynard, H. D., and Kasko, A. M. (2013) Synthesis of photodegradable macromers for conjugation and release of bioactive molecules. *Biomacromolecules 14*, 1199-1207.
24. Saran, D., and Burke, D. H. (2007) A versatile photocleavable bifunctional linker for facile synthesis of substrate-DNA conjugates for the selection of nucleic acid catalysts. *Bioconjugate Chem. 18*, 275-279.
25. Santos, T., Ferreira, R., Maia, J., Agasse, F., Xapelli, S., Cortes, L., Braganca, J., Malva, J. O., Ferreira, L., and Bernardino, L. (2012) Polymeric nanoparticles to control the differentiation of neural stem cells in the subventricular zone of the brain. *ACS Nano **6***, 10463-10474.
26. Maia, J., Santos, T., Aday, S., Agasse, F., Cortes, L., Malva, J. O., Bernardino, L., and Ferreira, L. (2011) Controlling the neuronal differentiation of stem cells by the intracellular delivery of Retinoic acid-loaded nanoparticles. *ACS Nano 5*, 97-106.
27. Solomek, T., Mercier, S., Bally, T., and Bochet, C. G. (2012) Photolysis of ortho-nitrobenzylic derivatives: the importance of the leaving group. *Photochem. Photobiol. Sci. 11*, 548-555.

28. Warrell Jr., R. P., Frankel, S. R., Miller Jr., W. H., Scheinberg, D. A., Itri, L. M., Hittelman, W. N., Vyas, R., Andreeff, M., Tafuri, A., Jakubowski, A., and et al. (1991) Differentiation therapy of acute promyelocytic leukemia with Tretinoin (*all-trans*-Retinoic acid). *N. Engl. J. Med. 324*, 1385-1393.
29. Thielitz, A., and Gollnick, H. (2008) Topical retinoids in acne vulgaris. *Am. J. Clin. Dermatol. 9*, 369-381.

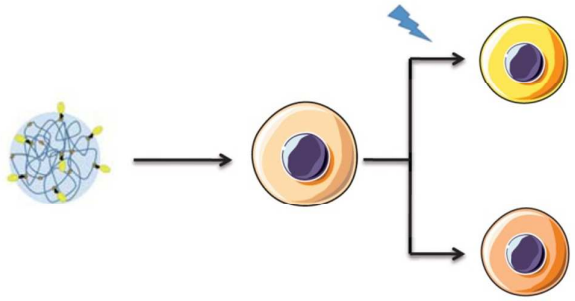

90x51mm (300 x 300 DPI)